Journal of
Plant Ecology

VOLUME 6, NUMBER 1,
PAGES 84–91

MARCH 2013

doi:10.1093/jpe/rts010

Advance Access publication
5 April 2012

available online at
www.jpe.oxfordjournals.org

Applicability of remote sensing-based surface temperature regimes in determining deciduous phenology over boreal forest

Quazi K. Hassan and K. Mahmud Rahman*

Department of Geomatics Engineering, University of Calgary, 2500 University Drive NW, Calgary, Alberta, Canada T2N 1N4
*Correspondence address. Department of Geomatics Engineering, University of Calgary, 2500 University Drive NW, Calgary, Alberta, Canada T2N 1N4. Tel: +1-403-210-9494; Fax: +1-403-284-1980;
E-mail: qhassan@ucalgary.ca

Abstract

Aims

The study of deciduous phenology over boreal forest is important for understanding forest ecology and better management. In this paper, our objective was to determine the phenological stages of deciduous leaf out (DLO) over the deciduous-dominant [i.e. trembling aspen (*Populus tremuloides*)] stands in the Canadian Province of Alberta.

Methods

During the period 2006–2008, we used Moderate Resolution Imaging Spectroradiometer (MODIS)-based 8-day surface temperature (T_S) images to calculate accumulated growing degree days (AGDD: a favourable temperature regime for plant growth). The temporal dynamics of AGDD in conjunction with *in situ* DLO observations were then analysed in determining the optimal threshold for DLO in 2006 (i.e. 80 degree days).

Important Findings

The implementation of the above-mentioned optimal threshold revealed reasonable agreements (i.e. on an average 91.9% of the DLO cases within ±2 periods or ±16 days of deviations during 2007–2008) in comparison to the *in situ* observed data. The developments could be useful in various forestry-related applications, e.g. plant growth and its ability of exchanging atmospheric carbon dioxide, forest ecohydrology, risk of insect infestation, forest fire and impact of climate change, among others.

Keywords: accumulated growing degree days • deciduous leaf out • enhanced vegetation index • Moderate Resolution Imaging Spectroradiometer

Received: 26 August 2011 Revised: 3 March 2012 Accepted: 11 March 2012

INTRODUCTION

Vegetation phenology is the science of understanding the periodic/cyclic events associated with the plant developmental stages and mainly associated with climatic regimes (Delpierre *et al.* 2009; Morisette *et al.* 2009). Over boreal ecosystems, the phenological stages of deciduous tree/plant(s) can broadly be grouped into the categories of (i) bud burst (ii) deciduous leaf out (DLO), (iii) maximum green-up, (iv) leaf senescence timing, (v) deciduous leaf fall and (vi) commence of snowfall (Delbart *et al.* 2006; Delpierre *et al.* 2009; Duchemin *et al.* 1999; Hanes and Schwartz 2010; McCloy 2010; Reed *et al.* 2009). In general, these stages provide valuable information regarding: (i) plant growth (Hari and Nojd 2009), (ii) plants' ability of exchanging atmospheric carbon dioxide (Cleland *et al.* 2007), (iii) forest ecohydrology, e.g. evapotranspiration, precipitation, soil moisture, canopy moisture, etc. (Wilson and Baldocchi 2000) and (iv) risk of insect infestation (Hogg 1999), among others.

The most accurate and widely used method of determining the deciduous phenological stages is the employment of *in situ* observations (Beaubien and Hamann 2011; White *et al.* 2009). Despite its accuracy, it only provides site-specific information over relatively smaller geographical extent (several hundreds of square metres). Thus, in order to address the spatial dynamics over a large area, it requires alternate approaches. In this context, remote sensing-based methods can be such an alternate, which have already been proven as an effective technological advancement in determining various phenological stages over various biomes across the world (Cleland *et al.*

2007; Delbart *et al.* 2006; Morisette *et al.* 2009; Reed *et al.* 2009; White *et al.* 2009).

In most of the instances, remote sensing-based vegetation and water content indices are commonly used ones in determining various vegetation developmental stages, e.g. green-up, maturity, etc. Those include the application of (i) normalized difference vegetation index (NDVI: a measure of vegetation greenness) in determining the onset of green-up over temperate deciduous broadleaf forests in France (Duchemin *et al.* 1999; Soudani *et al.* 2008) and boreal forest in northern Eurasia (Delbart *et al.* 2006), (ii) enhanced vegetation index (EVI: a measure of vegetation greenness and canopy structure; Huete *et al.* 2002) in determining the onset of green-up over deciduous broadleaf forest in USA (Ahl *et al.* 2006; Liang *et al.* 2011) and boreal-forested regions in Canada (Sekhon *et al.* 2010), (iii) leaf area index (LAI: a measure of one-sided green leaf area per unit ground area; Chen and Black 1992) in defining the vegetation maturity over mixed temperate deciduous forest in USA (Hanes and Schwartz 2010) and (iv) normalized difference water index (NDWI: a measure of water/moisture in the canopy) in defining the DLO over boreal forest in central Siberia (Delbart *et al.* 2005); among others. The temporal trends of these indices are used for detecting the changes in biophysical and/or biochemical characteristics of the vegetation associated with the phenological stage (McCloy 2010; Xiao *et al.* 2009). Recent studies suggest that the application of both NDVI and EVI in predicting the spring onset induces uncertainty due to the presence of snow on the ground over the boreal-dominant regions in particular (Delbart *et al.* 2006; Sekhon *et al.* 2010). Thus, we may assume that the application of LAI also may be affected in a similar fashion. On the other hand, the implementation of NDWI reveals that it is capable of determining the vegetation developmental phases independent of the snow conditions (Delbart *et al.* 2006; Reed *et al.* 2009; Sekhon *et al.* 2010). In general, the temporal trends of these indices are able to determine several phenological stages, such as onset, maturity and end of the growing season depending on the type of the forested ecosystems (Delbart *et al.* 2005; Zhang *et al.* 2003). However, some of the intermediate phenological stages (e.g. DLO) during the growing season may require further investigation.

In general, the responses of vegetation are largely controlled by the climatic variables (Hassan and Bourque 2009); while remote sensing-based surface temperature (T_S) products have been used to determine deciduous phenology, it has been limited in use. For example: (i) Hanes and Schwartz (2010) determined the dynamics of leaf out in a deciduous-dominant mixed temperate deciduous forest in USA as a function of accumulated growing degree days (AGDD: defined as the favourable temperature regime for plant growth) and (ii) Zhang *et al.* (2004) determined the green-up onset as a function of accumulated chilling days (i.e. days with temperatures experiencing less than a threshold value) in the northern hemisphere between 35 and 70°N. In both of the above cases, Moderate Resolution Imaging Spectroradiometer (MODIS)-based T_S products were directly used without transforming them into equivalent daily average air temperature. As, for the calculation of growing degree days (GDD) and chilling days, it would be very common to use such average air temperature measured near the surface (Li *et al.* 2010). In this context, the GDD mapping methods (as described in Akther and Hassan 2011; Hassan *et al.* 2007a, 2007b) using MODIS-based T_S products in conjunction with ground-based air temperature measurements would be a viable alternate.

In this paper, our overall goal was to determine the deciduous phenological stage of DLO associated with trembling aspen (*Populus tremuloides*) using MODIS-based T_S images over the boreal-dominant-forested regions in the Canadian Province of Alberta. The specific objectives were to (i) determine AGDD threshold for predicting DLO at lookout tower sites (for location information see Fig. 1) during 2006, (ii) implement the observed threshold in objective (a) during the period 2007–2008 and compare the predictions with the observed values at the lookout tower sites and (iii) generate DLO maps and discuss their spatial dynamics.

MATERIALS AND METHODS

General description of the study area

We considered the Canadian Province of Alberta as our study area, which lies in between 49–60°N latitude and 110–120°W longitude (Fig. 1). Topographically, the relief ranges from 150 to 3650 m above mean sea level. Climatically, it experiences relatively humid conditions (i.e. annual precipitation in the range 260–1710 mm) with short summers, long and cold winters (where the average annual temperature in the range −7.1 to 6°C) (Dowing and Pettapiece 2006). The province is divided into six natural regions on the basis of climate, soil and vegetation types; and their brief descriptions are provided in Table 1. Among the forest-dominant regions, the most dominant deciduous species are found to be trembling aspen and balsam poplar (*Populus balsamifera*) (Li *et al.* 2010). The spatial distribution of the deciduous-dominant stands in the province at 30 m spatial resolution was obtained from Alberta Sustainable Resource Development (SRD) (see the grey shades in Fig. 1a) and the dynamics of DLO were only determined within the deciduous-dominant stands. However, this map was resampled to 500 m spatial resolution to align with the MODIS data set. In this process, we employed dominant method for the up-scaling, which was based on counting dominant values (in this case deciduous-dominant stands) within 17 × 17 window (i.e. ~500 m × 500 m) of the original map. In the resultant map, we found negligible changes (i.e. <1%) in the total area in comparison to the original map.

In situ phenological and air temperature data

We obtained phenological data for DLO at the lookout tower sites (marked with black circles in Fig. 1) available from Alberta

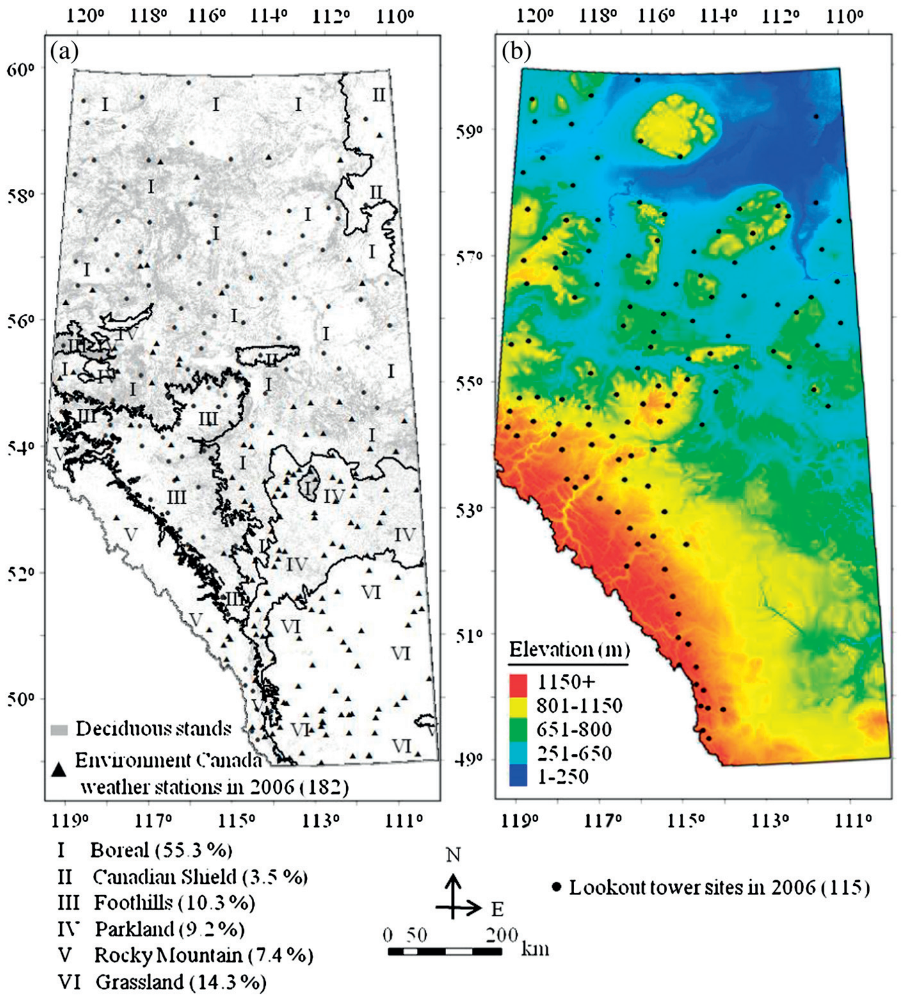

Figure 1: (**a**) map of Alberta showing the location of (i) Environment Canada weather stations where the daily average air temperature was acquired at a height between 1.2 and 2 m above the ground surface and (ii) lookout tower sites where DLO *in situ* observations were acquired, along with the boundaries of the natural regions. (**b**) digital elevation model of Alberta along with the location of lookout tower sites.

Table 1: brief description of the study area after Dowing and Pettapiece (2006)

Natural region no.	Natural region name	% of Alberta	Mean annual temperature (°C)	Mean annual precipitation (mm)	Main vegetation coverage	Number of lookout towers (2006)
I	Boreal	55.3	−0.2	469	Mixedwood: dominant aspen, white sprue and black sprue, shrubby understories, jack pine	68
II	Canadian Shield	3.5	−2.6	380	Rock barrens (mixed with aspen, open jack pine, birch), dry jack pine forests, dunes largely unvegetated	3
III	Foothills	10.3	1.7	603	Mainly closed coniferous forests (aspen-lodgepole pine, lodgepole pine-black spruce, white spruce)	33
IV	Parkland	9.2	2.3	447	Aspen forests with grass lands	0
V	Rocky Mountain	7.4	−0.4	798	Mixed aspen and conifer forests (lodgepole pine, white spruce, douglas fir)	11
VI	Grassland	14.3	4	374	Grasslands (blue grama, needle and thread), shrublands	0

SRD during the period 2006–2008. The DLO stage was defined as the time when 75% or more of the leaves would open with a length of at least 1.25 cm in diameter for the trembling aspen trees in the surrounding area of a lookout tower sites (FFMT 1999). The number of lookout tower sites was ~110 per year and these were spanning approximately in the (i) elevation range 350–2500 m and (ii) latitude range 49–60°N. In general, we observed that the timing of DLO increased from low to high latitudes and/or elevations. These data were recorded in the form of day of year (DOY: 1–365 or 366 depending on the leap year), thus we transformed them into equivalent 8-day period coinciding with that of MODIS 8-day composites using the following expression (Sekhon *et al.* 2010):

$$P = \left(\frac{\text{DOY} - 1}{8}\right) + 1, \quad (1)$$

where P (=1–46) is the equivalent number of periods that falls during the MODIS 8-day composites, and always, it will be an integer (e.g. P = 24 if the Eq. 1 produces values in the range 24.125–24.875). Upon implementation, we observed the average period of DLO was the 18th period for the years 2006–2008.

We also obtained daily average air temperature acquired at 1.2–2 m above the surface at 182 weather stations (for location information see Fig. 1) during the years 2006–2008, available from Environment Canada. These data were averaged at 8-day intervals, which also had to coincide with the MODIS 8-day composites. Both of the phenological and air temperature data sets were employed in calibrating and validating MODIS-based estimations of DLO stage.

Satellite data and their processing

We used MODIS-based data available from NASA during the growing seasons (i.e. April–October) for the years 2006–2008. These included (i) 8-day composites of T_S (i.e. MOD11A2 V.005) at 1 km spatial resolution and (ii) 8-day composites of surface reflectance (MOD09A1 V.005), which were then used to calculate EVI at 500 m spatial resolution using the following expression (Huete *et al.* 2002):

$$\text{EVI} = 2.5\frac{\rho_{\text{NIR}} - \rho_{\text{Red}}}{\rho_{\text{NIR}} + 6\rho_{\text{Red}} - 7.5\rho_{\text{Blue}} + 1}, \quad (2)$$

where ρ is the surface reflectance for the near infrared (NIR), red and blue spectral bands. We preferred to calculate the EVI images at 8-day intervals to match the temporal resolution of the T_S images instead of MODIS EVI products (i.e. MOD13Q1 V.005, only available in the form of 16-day composites). Both of the data sets (i.e. T_S and EVI) were used to calculate GDD by adopting the empirical methods described in Akther and Hassan (2011). It consisted of several steps:

(i) We extracted the MODIS-based instantaneous 8-day composites of T_S at each of the single pixels (i.e. acquired between 10:30 and 12:00 local time) at the 182 weather stations and compared them with the 8-day average air temperature ($\bar{T}_a$) during 2006 (Fig. 2a).

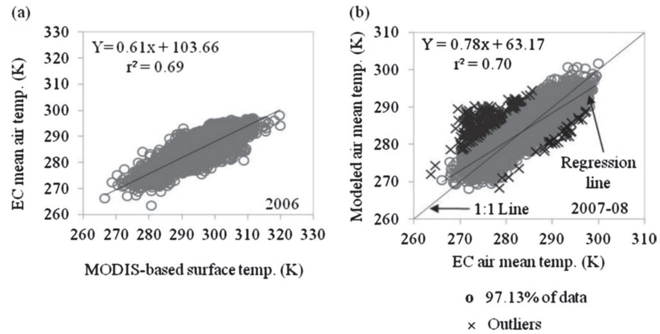

Figure 2: (**a**) relation between MODIS-based 8-day composites of instantaneous surface temperature (acquired between 10:30–12:00 local time) and 8-day average air temperature obtained from Environment Canada in 2006 (n = 4561; F-statistics = 10 071.80 with P value < 0.0001) and (**b**) validation of the relationship as seen in (a) during 2007–2008 (n = 8594; F-statistics = 20 288.79 with P value < 0.0001).

(ii) In order to validate the observed relation in Step (i), we used it at the sites of the same 182 weather stations during the years 2007–2008 and compared with the $\bar{T}_a$ (Fig. 2b).
(iii) We then applied the observed relation in Fig. 2a in converting the MODIS-based T_S images into equivalent $\bar{T}_a$. These were then used to calculate GDD maps at 1 km spatial resolution using the following expression (Heidi and Ari 2008):

$$\text{GDD} = \overline{T_a} - T_{\text{base}}, \quad (3)$$

where T_{base} is the base temperature (=278.15 K), which is considered to be the minimum requirement for plant growth in our study area (Dowing and Pettapiece 2006; Hassan *et al.* 2007b). (iv) We implemented a data fusion technique initially described in Hassan *et al.* (2007a) in enhancing the spatial resolution of GDD maps from 1 km to 500 m using EVI images as a basis of fusion. It was possible as GDD and EVI were found to be linearly correlated (i.e. r^2 = 0.87; Hassan *et al.* 2007b). Mathematically, the data fusion process could be expressed as follows (Hassan *et al.* 2007a):

$$\text{GDD}_{500\,\text{m}} = \frac{\text{EVI}_{\text{ins}}}{\text{EVI}_{\text{avg}}} \times \text{GDD}_{1\,\text{km}}, \quad (4)$$

where EVI_{ins} is the instantaneous value of EVI at the centre of a 3 × 3 moving window, EVI_{avg} is the average value of all of the EVI values within the moving window. The ratio between EVI_{ins} and EVI_{avg} acts as a weighted function in the calculation of GDD at 500 m resolution. (v) At each of the period, we calculated AGDD using the following expression:

$$\text{AGDD} = \sum_{i=1}^{n} (8 \times \text{GDD}_{500\,\text{m}}), \quad (5)$$

where i is the first 8-day period of the growing season and n (=1–27) is the 8-day period of interest during the growing season.

Determining DLO threshold and its implementation

During the years of 2006–2008, we extracted the temporal trends of both GDD and AGDD at the lookout tower sites with available *in situ* DLO records. For the determination of DLO threshold, we divided the data set into calibration and validation ones. We used ~34% data points (i.e. during 2006) in calibration and the remaining ~66% data points (i.e. during 2007–2008) in validation purposes. We performed the calibration for DLO in two distinct steps:

(i) Calculated the average and standard deviation (SD) of AGDD during the average *in situ* DLO observation period. The observed average AGDD value was then considered as an initial 'threshold' for DLO determination (i.e. either equal or greater amount of AGDD would be the minimum requirement for DLO occurrence).
(ii) Performed sensitivity analysis for the initial threshold in determining the DLO stage in the range 'initial threshold ± 1 SD'. The optimal threshold was then determined when the deviations between the predicted and observed DLO period would be reasonable for the most of the cases (for more details, see 'Results' section and Table 2). In terms of illustrating early and delayed predictions with compare to the *in situ* DLO observation periods, we used the signs of '−' and '+' deviations, respectively, throughout the manuscript.

In the scope of validation, we predicted the periods for DLO during the years 2007–2008 using the optimal threshold observed in the calibration phase as discussed above. We then calculated the deviations between the predicted and observed DLO periods in determining the agreements between the data sets (for more details, see 'Results' section and Table 3). Finally, we generated the spatial dynamics of DLO using the optimal threshold over the deciduous-dominant stands shown in Fig. 1.

Table 2: implementation of different AGDD thresholds in determining the optimal threshold by evaluating the deviations between observed and predicted DLO periods at each of the lookout tower sites using the data from 2006

% of 115 lookout towers (2006)								
	Deviations (in periods)							
AGDD threshold	0	±1	±2	±3	±4	±5	±6	±7
60	30.4	87.8	98.3	99.1	99.1	99.1	99.1	100
70	31.3	87.8	98.3	99.1	99.1	99.1	100	100
80	**35.7**	**86.1**	**98.3**	**99.1**	**99.1**	**99.1**	**100**	**100**
90	39.1	80.9	94.8	99.1	99.1	99.1	100	100
100	34.8	73.9	92.2	98.3	99.1	99.1	100	100
110	33.0	67.8	87.0	96.5	99.1	99	100	100
120	27.8	60.9	81.7	93.0	98.3	98	100	100
130	20.9	53.9	77.4	91.3	97.4	97	100	100
140	13.9	47.0	68.7	89.6	97.4	97	100	100

The bold row indicates the optimal threshold and its performance.

RESULTS

Relation between MODIS-based T_S and 8-day average air temperature

The relation between MODIS-based instantaneous 8-day composites of T_S and 8-day average air temperature ($\bar{T}_a$) during 2006 revealed reasonably strong relations (i.e. $r^2 \approx 0.69$ with a slope of 0.61 ± 0.01 and intercept of 103.66 ± 3.55 at 95% confidence level for the regression line with P value < 0.0001; Fig. 2a). We observed a similar relationship (i.e. $r^2 \approx 0.70$ with a slope of 0.78 ± 0.01 and intercept 63.17 ± 3.05 at 95% confidence level for the regression line with P value < 0.0001; Fig. 2b) for ~97% of the cases during 2007–2008 period. The remaining 2.87% of the data points (i.e. 254 of 8848) were found to be in southern Alberta, where the land cover is primarily agriculture area and therefore excluded from the above-mentioned analysis. Note that similar agreements (i.e. $r^2 \approx 0.70$) were also observed in other studies (Akther and Hassan 2011).

Determination of DLO threshold and its validation

Fig. 3a illustrates the averaged temporal trends of GDD and AGDD during 2006 upon considering all of the 115 lookout tower sites. We found that the initial AGDD threshold was 101 degree days with a SD of ±40 degree days during the period of *in situ* DLO as shown with the vertical dotted line in Fig. 3a. We then analysed the distribution of the individual AGDD thresholds (Fig. 3b); ~ 82% of the cases were found to be in the range 60–140 degree days (i.e. ~initial threshold ± 1 SD). Due to the observed variability's in the individual AGDD thresholds, we performed a sensitivity analysis for the range 60–140 degree days (Table 2). We decided that the threshold of 80 would be the optimal selection; which yielded 35.7, 86.1, and 98.3% agreements at 0, ±1, and ±2 deviations, respectively. Note that AGDD threshold of 90 had the highest agreements at 0 deviation (i.e. 39.1% of the cases); however, relatively less for both ±1 (i.e. 80.9%) and ±2 (i.e. 94.8%) deviations. On the other hand, both of the AGDD thresholds of 60 and 70 showed greater agreements (i.e. 87.4%) at ±1 deviation but relatively less at ±0 deviation (i.e. ~31%) with compare to the threshold of 80. Upon applying the optimal AGDD threshold (i.e. 80 degree days) during the years 2007–2008 at the lookout tower sites, we found that the deviations were ±2 periods for significant portions of the cases (i.e. 94.5% in 2007, 89.4% in 2008; Table 3).

Spatial dynamics of DLO

Fig. 4 shows the spatial dynamics of DLO over the deciduous-dominant stands across Alberta during 2008 upon applying the observed optimal threshold of AGDD. It revealed that the DLO occurred during the periods 17–19 (i.e. 8–31 May 2008) for ~85% of the cases (Fig. 4).

Table 3: relation between observed and predicted DLO periods at each of the lookout tower sites during 2007–2008 using the optimal AGDD threshold of 80 degree days

		Deviations (in periods)						
Year	Number of lookout tower sites (*n*)	0	±1	±2	±3	±4	±5	±6
2007	110	30.9	78.2	94.5	98.2	99.1	100	100
2008	113	37.2	81.4	89.4	93.8	97.3	98.2	100
2007–2008	223	34.1	79.8	91.9	96.0	98.2	99.1	100

The '+ve' and '−ve' signs represent positive (i.e. delayed) and negative (i.e. early) predictions, respectively.

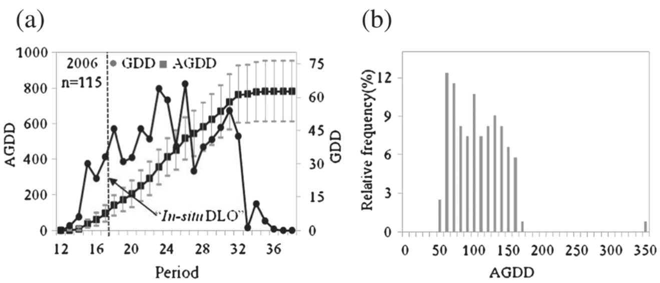

Figure 3: determination of DLO threshold: (**a**) averaged temporal trends of GDDs and AGDD during 2006 and the average *in situ* DLO observation period and (**b**) relative frequency distribution of all of the AGDD values at each individual lookout tower sites.

DISCUSSION

AGDD threshold for determining DLO

The variability in AGDD (i.e. ~82% of the cases in between 60 and 140 degree days) thresholds during the calibration phase (Fig. 3b) might be related with one or more of the following causes:

(i) Apart from the temperature regimes, the phenological stages would also be influenced by other climatic variables, e.g. photosynthetically active radiation and water regimes, which were not considered in the scope of this study.
(ii) Some other climatic condition during the prior winter season, i.e. the fulfilment of the chilling requirements would also a critical parameter (Morin *et al.* 2009).
(iii) It would be possible that the optimal amount of nutrient might not be available for all of the lookout tower sites.
(iv) Biological factors, such as the inter- and intra-species competition, were not take into consideration.
(v) The differences in genetic compositions among the inter- and intra-species might differ in terms of their growth requirements observed in other studies (Li *et al.* 2010), among others.

Upon analysing the sensitivity of the AGDD threshold (for details see Table 2), we found the optimal threshold (i.e. 80 degree days). This AGDD threshold was found to be similar (i.e. in the range 80–100 degree days) when compared to other studies conducted over western Canadian boreal forests (Barr *et al.* 2004; Parry *et al.* 1997).

During the DLO validation phase, the relatively high deviations (i.e. >±2 periods) between the MODIS-predicted and *in situ* observations were found to be ~10% of the cases. These were attributed due to the following reasons:

(i) The *in situ* measurements were on the basis of visual observations, thus, the operators' interpretation skills would be critical (Sekhon *et al.* 2010).
(ii) At each of the lookout tower sites, ~20 to 100 trees were sampled to define the occurrence of the phenological stage of interest (Dylan Heerema: a veteran lookout tower operator, personal communication). Thus, it would be possible that the spatial resolution of the *in situ* observations might not have similar dimension as of MODIS data for some cases.
(iii) One global threshold might not be able to delineate the entire spatial dynamics across the study area (Li *et al.* 2010).

Robustness of AGDD threshold

The optimal threshold of AGDD (i.e. 80 degree days) for DLO was determined using the calibration data from the year 2006 and then evaluated using the validation data from the period 2007 to 2008. The observed agreements in calibration (i.e. ~98.3% of the cases) and validation (i.e. ~91.9% of the cases) phases were similar. Despite these reasonable agreements, it would be important to investigate how robust these thresholds under various climatic conditions (e.g. dry, normal and wet years). Such climatic conditions in comparison to long-term average data during the period 1960–2007 were reported by Alberta Department of Agriculture and Rural Development (ACIS 2009) and summarized over the forested regions as follows:

(i) During 2006, the climatic conditions were spanning from dry to wet, e.g. some areas in northeast, northwest and southwest were having dry conditions.
(ii) The year 2007 was mostly near normal to wet except some pockets of dry areas in northeast and southwest
(iii) The year 2008 was mostly dry except some pockets.

Spatial dynamics of DLO

In terms of the spatial dynamics of DLO stage, we observed the following generalized patterns:

(i) The occurrence of DLO was found to be relatively earlier (⩽16 period, i.e. before 8 May 2008) primarily in the natural

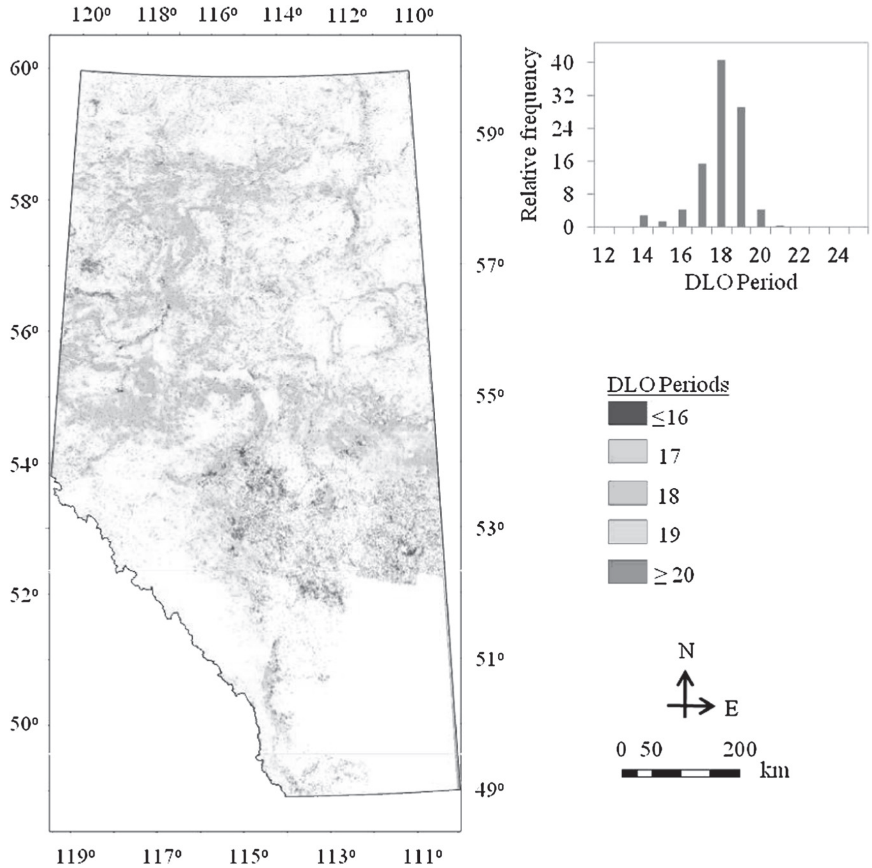

Figure 4: spatial dynamics for the timing of DLO and its relative frequency during 2008.

region of parkland and also along the river bodies. These are related to the fact that these regions experience relatively warm temperature regimes (Dowing and Pettapiece 2006).
(ii) The timing of DLO occurrence happened to be delayed towards northward directions. This would be related to the fact that temperature regimes decrease in the northward directions in the northern hemisphere (Hassan *et al.* 2007b; Sekhon *et al.* 2010).

Contributions

In the scope of this paper, we studied a topical theme, i.e. application of remote sensing in understanding vegetation phenology. However, it would be worthwhile to note that the proposed methodology (i.e. integration of MODIS-based T_S and EVI products) is unique in mapping the beginning (i.e. leaf outing) of the growing season for the deciduous-dominant stands over boreal-forested regions. Apart from the general applications of phenological stages mentioned in the first paragraph of 'Introduction' section, we believe that the DLO stages could also be important in (i) understanding forest fire danger conditions, (ii) modelling of forest fire behaviour in the event of fire occurrences and (iii) quantifying the impact of climate change (Cleland *et al.* 2007), among others.

CONCLUDING REMARKS

Here, we demonstrated the potential of MODIS-based AGDD in determining the phenological stage of DLO over the boreal-forested regions in Alberta. It revealed that the DLO could be determined with reasonable agreements (i.e. within ±2 periods or ±16 days of deviations) for 91.9% of the cases. The proposed methods would be useful in delineating DLO stage in the remote areas of the landscape, where the *in situ* observations would be difficult. However, it would be worthwhile to mention that the suitability of the optimal AGDD (i.e. 80 degree days) should be evaluated against longer time period.

FUNDING

This study was partially supported by an National Sciences and Engineering Research Council of Canada (NSERC) Discovery Grant provided to Q.K.H.

ACKNOWLEDGEMENTS

The authors would like to acknowledge: (i) NASA for providing the MODIS data, (ii) Alberta SRD for providing *in situ* DLO observation data and (iii) Environment Canada for providing air temperature data.
Conflict of interest statement. None declared.

REFERENCES

AgroClimatic Information Service (ACIS) (2009) *Precipitation Historical Summaries (1961 to 2008) Thumbnails (12 Maps per Page) Yearly Relative to Normal 1997 to 2008*. Alberta, Canada: Alberta Agriculture and Rural Development. http://www.agric.gov.ab.ca/app116/acis/quick/largeMap.jsp (24 November 2011, date last accessed).

Ahl DE, Gower ST, Burrows SN, Shabanov NV, *et al.* (2006) Monitoring spring canopy phenology of a deciduous broadleaf forest using MODIS. *Remote Sens Environ* **104**:88–95.

Akther MS, Hassan QK (2011) Remote sensing based estimates of surface wetness conditions and growing degree days over northern Alberta, Canada. *Boreal Environ Res* **16**:407–16.

Barr AG, Black TA, Hogg EH, *et al.* (2004) Inter-annual variability in the leaf area index of a boreal aspen-hazelnut forest in relation to net ecosystem production. *Agric For Meteorol* **126**:237–55.

Beaubien EG, Hamann A (2011) Plant phenology networks of citizen scientists: recommendations from two decades of experience in Canada. *Int J Biometeorol* 10.1007/s00484-011-0457-y.

Chen JM, Black TA (1992) Defining leaf area index for non-flat leaves. *Agric For Meteorol* **57**:1–12.

Cleland EE, Chuine I, Menzel A, *et al.* (2007) Shifting plant phenology in response to global change. *Trends Ecol Evol* **22**:357–65.

Delbart N, Kergoata L, Toana TL, *et al.* (2005) Determination of phenological dates in boreal regions using normalized difference water index. *Remote Sens Environ* **97**:26–38.

Delbart N, Toan TL, Kerogoats L, *et al.* (2006) Remote sensing of spring phenology in boreal regions: a free of snow-effect method using NOAA-AVHRR and SPOT-VGT data (1982-2004). *Remote Sens Environ* **101**:52–62.

Delpierre N, Dufrene E, Soudani K, *et al.* (2009) Modeling interannual and spatial variability of leaf senescence for three deciduous tree species in France. *Agric For Meteorol* **149**:938–48.

Dowing DJ, Pettapiece WW (2006) *Natural Regions and Subregions of Alberta*. Albert, Canada: Publication T/852, Natural Regions Committee, Government of Alberta.

Duchemin B, Goubier J, Courrier G (1999) Monitoring phenological key stages and cycle duration of temperate deciduous forest ecosystems with NOAA/AVHRR Data. *Remote Sens Environ* **67**:68–82.

Forest Fire Management Terms (FFMT) (1999) *Forest Protection Division*. Alberta, Canada: Alberta Land and Forest Service, 77. http://www.srd.alberta.ca/MapsFormsPublications/Publications/documents/ForestFireManagementTerms-AbbrevGlossary (11 October 2010, date last accessed).

Hanes JM, Schwartz MD (2010) Modeling land surface phenology in a mixed temperate forest using MODIS measurements of leaf area index and land surface temperature. *Theor Appl Climatol* 10.1007/s00704-010-0374-8.

Hari P, Nojd P (2009) The effect of temperature and PAR on the annual photosynthetic production of Scots pine in northern Finland during 1906-2002. *Boreal Environ Res* **14**:5–18.

Hassan QK, Bourque CP-A (2009) Potential species distribution of balsam fir based on the integration of biophysical variables derived with remote sensing and process-based methods. *Remote Sens* **1**:393–407.

Hassan QK, Bourque CP-A, Meng F-R (2007*a*) Application of Landsat-7 ETM+ and MODIS products in mapping seasonal accumulation of growing degree days at an enhanced resolution. *J Appl Remote Sens* **1**:013539.

Hassan QK, Bourque CP-A, Meng F-R, *et al.* (2007*b*) Spatial mapping of growing degree days: an application of MODIS-based surface temperatures and enhanced vegetation index. *J Appl Remote Sens* **1**:013511.

Heidi T, Ari V (2008) The relationship between fire activity and fire weather indices at different stages of the growing season in Finland. *Boreal Environ Res* **13**:285–302.

Hogg EH (1999) Simulation of interannual responses of trembling aspen stands to climatic variation and insect defoliation in western Canada. *Ecol Model* **114**:175–93.

Huete A, Didan K, Miura T, *et al.* (2002) Overview of the radiometric and biophysical performance of the MODIS vegetation indices. *Remote Sens Environ* **83**:195–213.

Li H, Wang X, Hamann A (2010) Genetic adaptation of aspen (*Populus tremuloides*) populations to spring risk environments: a novel remote sensing approach. *Can J For Res* **40**:2082–90.

Liang L, Schwartz MD, Fei S (2011) Validating satellite phenology through intensive ground observations and landscape scaling in a mixed seasonal forest. *Remote Sens Environ* **115**:143–57.

McCloy KR (2010) Development and evaluation of phenology changes indices derived from time series of image data. *Remote Sens* **2**:2442–73.

Morin X, Lechowicz MJ, Augspurger C, *et al.* (2009) Leaf phenology in 22 North American tree species during the 21st century. *Glob Change Biol* **15**:961–75.

Morisette JT, Richardson AD, Knapp AK, *et al.* (2009) Tracking the rhythm of the seasons in the face of global change: phenological research in the 21st century. *Front Ecol Environ* **7**:253–60.

Parry D, Volney WJA, Currie CR (1997) The relationship between trembling aspen phenology and larval development of the large aspen tortrix. *Information Report NOR-X-350*. Edmonton, Canada: Natural Resources Canada, Canadian Forest Service, Northern Forestry Centre.

Reed BC, Schwartz MD, Xiao X (2009) Remote sensing phenology: status and the way forward. In: Noormets A (ed). *Phenology of Ecosystem Processes*. New York: Springer Sciences+Business Media, 231–46.

Sekhon NS, Hassan QK, Sleep RW (2010) Evaluating potential of MODIS-based indices in determining ''snow gone'' stage over forest-dominant regions. *Remote Sens* **2**:1348–63.

Soudani K, Maire GL, Dufrene E, *et al.* (2008) Evaluation of the onset of green-up in temperate deciduous broadleaf forests derived from Moderate Resolution Imaging Spectroradiometer (MODIS) data. *Remote Sens Environ* **112**:2643–55.

White MA, De Beurs KM, Didan K, *et al.* (2009) Intercomparison, interpretation, and assessment of spring phenology in North America estimated from remote sensing for 1982–2006. *Glob change Biol* **15**:2335–59.

Wilson KB, Baldocchi DD (2000) Seasonal and interannual variability of energy fluxes over a broadleaved temperate deciduous forest in North America. *Agric For Meteorol* **100**:1–18.

Xiao X, Zhang J, Yan H, *et al.* (2009) Land surface phenology: convergence of satellite and CO_2 eddy flux observations. In: Noormets A (ed). *Phenology of Ecosystem Processes*. New York: Springer Sciences+Business Media, 247–70.

Zhang X, Friedl MA, Schaff CB, *et al.* (2003) Monitoring vegetation phenology using MODIS. *Remote Sens Environ* **84**:471–5.

Zhang X, Friedl MA, Schaff CB, *et al.* (2004) Climate controls on vegetation phenolgical patterns in northern mid- and high latitudes inferred from MODIS data. *Glob Change Biol* **10**:1133–45.